PHILOSOPHICAL TRANSACTIONS OF THE ROYAL SOCIETY A MATHEMATICAL, PHYSICAL & ENGINEERING SCIENCES

Null Field Approach to Scalar Diffraction. II. Approximate Methods

R. H. T. Bates and D.J. N. Wall

Phil. Trans. R. Soc. Lond. A 1977 **287**, 79-95
doi: 10.1098/rsta.1977.0140

Phil. Trans. R. Soc. Lond. A. **287**, 79–95 (1977) [79]
Printed in Great Britain

NULL FIELD APPROACH TO SCALAR DIFFRACTION
II. APPROXIMATE METHODS

BY R. H. T. BATES† AND D. J. N. WALL‡
† *Electrical Engineering Department, University of Canterbury, Christchurch, New Zealand*
‡ *Mathematics Department, University of Dundee, Dundee, Scotland DD1 4HN*

(*Communicated by D. S. Jones, F.R.S. – Received* 9 *October* 1975 – *Revised* 26 *January* 1977)

CONTENTS

We develop from our generalized null field method a generalization of the Kirchhoff, or physical optics, approach to diffraction theory. Corresponding to each particular null field method there is a corresponding physical optics approximation, which becomes exact when one of the coordinates being used is constant over the surface of the scattering body. We show how to improve these approximations by a computational procedure which is more efficient than those introduced in the previous paper. The reradiations from our physical optics surface sources more nearly satisfy the extinction theorem the deeper they penetrate the interiors of scattering bodies. We find that we have to introduce a new definition of the parts of a body's surface that are directly illuminated and shadowed, and we suggest that this may be more apposite in general than the usual definition. The computational examples presented herein indicate that useful approximations to surface source densities are obtained in the umbra and penumbra of bodies. These examples also show that our scattered fields are in several particulars superior to those obtained from the conventional Kirchhoff approach. It is important to choose that physical optics approximation most appropriate for the scattering body in question.

1. INTRODUCTION

This is the second in a series of three papers in which a computationally orientated approach to diffraction theory is developed from the optical exinction theorem (extended boundary condition). In the first paper (Bates & Wall 1977), which is henceforth referred to as (I), we presented

our general method. Here we develop a generalization of Kirchhoff's approximate approach to diffraction.

Bouwkamp (1954) recalls that when Kirchhoff was attempting to find tractable methods for calculating the diffraction of waves by a hole in a plane screen, he realized that he could obtain quite simple formulae if he were to assume that the field in the hole was identical with the field that would be there if the screen were removed. As is now well known, the diffracted fields calculated on the basis of this assumption are in useful agreement with experiment even when the dimensions of the hole are only moderate in comparison with the wavelength.

The success of Kirchhoff's approach led gradually to what is now called (by electrical engineers, at least) the physical optics approximation. It is assumed that the source density induced at any point on the surface of a totally reflecting scattering body is identical with that which would be induced in a totally reflecting infinite plane tangent to the body at the said point. An inevitable corollary to this is that it must be assumed that no sources are induced on those parts of the body's surface that are not directly illuminated by the incident field. Thus, physical optics is a 'geometric optics' type of approximation, and it is sometimes loosely referred to as geometric optics, which is a pity because physical optics predicts several diffraction effects quite adequately whereas conventional geometric optics does not. From now on we choose to give physical optics the name 'planar physical optics' because it is exact when the scattering body becomes an infinite plane. Bechmann & Spizzichino (1963, Ch. 3) show that planar physical optics source densities can be usefully postulated on the surfaces of penetrable bodies.

Planar physical optics is a 'local' theory – when calculating the surface source density at any point we only have to consider the incident field in a neighbourhood of the point, and it is only there that we have to take into account the shape of the body and its material constitution. It is a single-scattering approximation – in fact, it is a kind of Born approximation for scatterers with well-defined boundaries. It is an 'asymptotic' theory (cf. Kouyoumjian 1965). Ursell (1966) shows that it is exact for smooth, convex bodies in the limit of infinitely high frequencies. Crispin & Maffett (1965) point out that it gives remarkably accurate results for some bodies having linear dimensions not much larger than the wavelength. The chief secret of its success is that it usually predicts the scattered field most accurately where it is largest (e.g. 'specular' reflexions, cf. Senior 1965).

The main defects of planar physical optics are that it can violate reciprocity and it does not take account of multiple scattering.

We have discovered that the null field approach leads to a generalized physical optics, which becomes exact when the surface of the totally reflecting scattering body coincides with a surface on which the radial coordinate (of the coordinate system in which the particular null field method being used is expressed) is constant. We find that we obtain useful approximations to the surface source density in the penumbra and umbra of the body, something which planar physical optics is incapable of, by definition. There are no significant theoretical differences when we apply our ideas to sound-soft and sound-hard bodies. Consequently, we restrict this discussion to the former (its formulae are somewhat simpler and are, therefore, more readily understood). It is easy enough to write down the formulae for sound-hard bodies. The germs of our techniques are in a previous account (Bates 1968), but out present generalized approach is quite new.

In § 2 we quote the formulae of planar physical optics and develop our generalized physical optics from the generalized scalar null field method, itself developed in (I). We also give the formulae for cylindrical (circular and elliptic) physical optics because the illustrative examples

we present here are for cylindrical bodies (they can have any desired cross section). A numerically efficient procedure for making significant improvements to physical optics surface source densities is introduced in § 3.

Since physical optics is approximate, the radiations from physical optics surface sources do not satisfy the extinction theorem, i.e. at almost every point, P say, in the interior of a scattering body there is a finite difference between these radiations and the negative of the incident field. In § 4 we generalize a previous observation (Bates 1975*a*) that this difference tends to decrease as P penetrates deeper into the interior. In § 5 we present examples of surface source densities and scattered fields computed using the circular and elliptic physical optics approximations. We compare these computations with others obtained by inherently accurate techniques – i.e. the circular and elliptic null field methods, which are developed in (I) – and by planar physical optics. We evaluate the significance of our work in § 6.

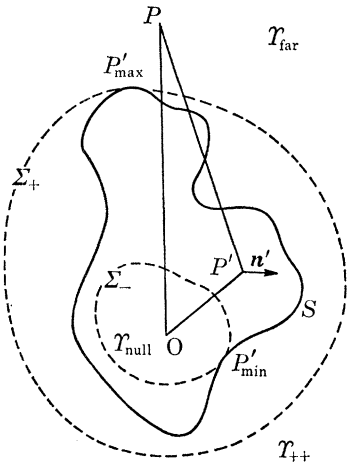

FIGURE 1. Totally reflecting scattering body of arbitrary shape.

2. GENERALIZED PHYSICAL OPTICS FOR SOUND-SOFT BODIES

Figure 1 shows the surface S of a totally reflecting body of arbitrary shape embedded in the three-dimensional space Υ, which is partitioned into Υ_- and Υ_+, the regions inside and outside S respectively. A point O, with Υ_-, is taken as origin for orthogonal curvilinear coordinates of a kind allowing the separation of the scalar Helmholtz equation. Arbitrary points in Υ and on S are denoted respectively by P, with coordinates (u_1, u_2, u_3), and P', with coordinates (u'_1, u'_2, u'_3). The coordinate n' describes the outward normal direction to S at P'. The surfaces Σ_- and Σ_+, on both of which the coordinate u_1 is constant, respectively inscribe and circumscribe S, in the sense that they are tangent to it but do not cut it. The points of tangency between Σ_- and S, and between Σ_+ and S, are $P'_{\min}$, and $P'_{\max}$. The values of u_1 at $P'_{\min}$ and $P'_{\max}$ are u'_{1-} and u'_{1+} respectively. The part of Υ_+ outside Σ_+ is denoted by Υ_{++}, and the part of Υ_- inside Σ_- is denoted by Υ_{null}. Other aspects of this notation are covered in § 2 of (I).

We now invoke formulae developed in §§ 2, 4 and 5 of (I). Table 1 of (I) should also be referred to. Recall that the null field approach is predicated upon the incident field ψ_0 being extinguished everywhere inside S by the scattered field ψ. We examine monochromatic fields and write

$$\psi_0 = \sum_{l=0}^{\infty} \sum_{j=-l}^{l} c_{j,l} a_{j\,l} \hat{j}_{j,l}(u_1, k)\, \hat{Y}_{j,l}(u_2, u_3, k), \quad P \in \Upsilon, \tag{2.1}$$

where the time factor $\exp(\mathrm{i}\omega t)$ is suppressed and k is the wave number. The $c_{j,l}$ are normalization constants appropriate for the particular coordinate system for which $\hat{\jmath}_{j,l}(\cdot)$ and $\hat{Y}_{j,l}(\cdot)$ are everywhere-regular radial and angular eigenfunctions. The $a_{j,l}$ are constants characterizing the form of the incident wave. Multipole expansions of the field ψ reradiated from the sources induced in the surface of the body are

$$\begin{aligned}\psi &= \sum_{l=0}^{\infty}\sum_{j=-l}^{l} c_{j,l}\, b^{-}_{j,l}\, \hat{\jmath}_{j,l}(u_1 k)\, \hat{Y}_{j,l}(u_2, u_3, k), \quad P \in \mathcal{Y}_{\mathrm{null}} \\ &= \sum_{l=0}^{\infty}\sum_{j=-l}^{l} c_{j,l}\, b^{+}_{j,l}\, \hat{h}^{(2)}_{j,l}(u_1, k)\, \hat{Y}_{j,l}(u_2, u_3, k), \quad P \in \mathcal{Y}_{++}, \end{aligned} \tag{2.2}$$

where the $\hat{h}^{(2)}_{j,l}(\cdot)$ are the 'outgoing' radial eigenfunctions, which are singular at $u_1 = 0$. Note should be taken of the functions and constants listed, for specific coordinate systems, in tables 2 through 4 and 6 of (I). The $b_{j,l}$, which depend upon k, ψ_0 and S, are given by

$$b_{j,l} = -\int_S\int f(\tau_1, \tau_2)\, K_{j,l}\, \mathrm{d}s, \tag{2.3}$$

where τ_1 and τ_2 are suitable parametric coordinates in S. Either a superscript $-$ or a superscript $+$ is affixed to both $b_{j,l}$ and $K_{j,l}(\cdot)$, the latter being defined by

$$K^{-}_{j,l} = \hat{h}^{(2)}_{j,l}(u'_1, k)\, \hat{Y}_{j,l}(u'_2, u'_3, k); \tag{2.4}$$

$$K^{+}_{j,l} = \hat{\jmath}_{j,l}(u'_1, k)\, \hat{Y}_{j,l}(u'_2, u'_3, k). \tag{2.5}$$

The null field equations for sound-soft bodies can be written as

$$b^{-}_{j,l} + a_{j,l} = 0 \quad (l \in \{0 \to \infty\};\, j \in \{-l \to l\}) \tag{2.6}$$

as follows from (4.2) of (I) and (2.3) and (2.4) of this paper.

The form of the scattered field in the Fraunhofer region (usually called 'far field' by electrical engineers) is usually of interest. It is often convenient to calculate the far scattered field by using the asymptotic form introduced in § 4 (*d*) of (I) to simplify the integral in (2.5) of (I). Denoting the position vectors (with respect to O) of P and P' by $\boldsymbol{r}$ and $\boldsymbol{r}'$ respectively, and writing $|\boldsymbol{r}| = r$, we find that

$$\psi = \frac{-\exp(-\mathrm{i}kr)}{4\pi r}\int_S\int f(\tau_1, \tau_2)\exp\{\mathrm{i}(\boldsymbol{r}'\cdot\boldsymbol{r})\, k/r\}\,\mathrm{d}s, \quad P \in \mathcal{Y}_{\mathrm{far}}, \tag{2.7}$$

where $\mathcal{Y}_{\mathrm{far}}$ is the part of $\mathcal{Y}_{++}$ which is far enough away from the body to be in the Fraunhofer region (remember that this becomes increasingly distant as the wavelength decreases).

We use a tilde to denote any quantity that is computed on the basis of a physical optics approximation, e.g. $\tilde{\psi}$ is the physical optics scattered field, and $\tilde{f}$ is the physical optics surface source density. It is not necessary to identify which type of physical optics is implied, since it is always clear from the context.

(*a*) *Planar physical optics*

When the incident field originates from a point, such as Q in figure 2, it is convenient to partition S into the part $\bar{S}_+$ which is directly illuminated by the source at Q, and the part $\bar{S}_-$ which is shadowed from it. We define $\bar{S}_\pm$ by stating that when $P' \in \bar{S}_+$ the straight line QP does not intersect S between Q and P, whereas when $P' \in \bar{S}_-$ the straight line QP' must intersect S between Q and P'. This is illustrated in figure 2.

The planar physical optics surface source density is defined to be

$$\begin{aligned} \tilde{f} &= 0, && P' \in \bar{S}_- \\ &= 2\,\partial\psi_0'/\partial n, && P' \in \bar{S}_+, \end{aligned} \tag{2.8}$$

where ψ_0' is the value of ψ_0 at P'.

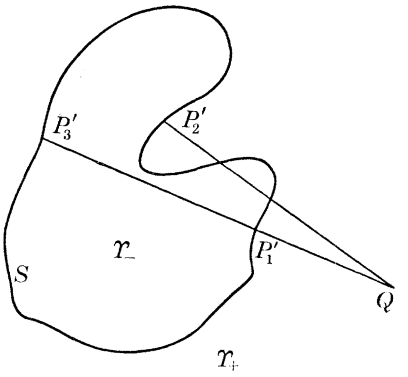

FIGURE 2. Directly illuminated and shadowed parts of S, for planar physical optics. Note that P_1' is on $\bar{S}_+$, whereas P_2' and P_3' are on $\bar{S}_-$.

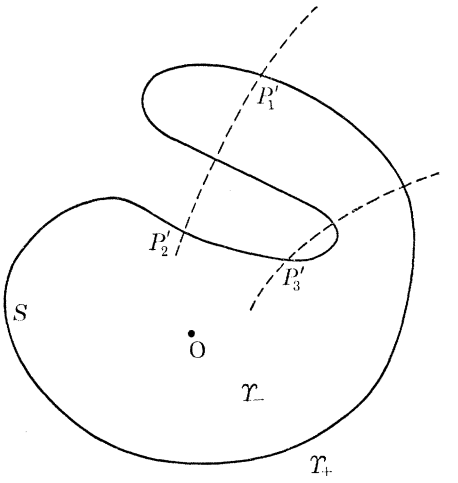

FIGURE 3. 'Directly illuminated' and 'shadowed' parts of S, for generalized physical optics. Note that P_1' is on S_+, whereas P_2' and P_3' are on S_-.

(*b*) *Generalized physical optics*

The true surface source density is not identically zero on $\bar{S}_-$, as defined in § 2 (*a*) above. The new approximate theory introduced here becomes exact for certain finite bodies. So we need different definitions of 'directly illuminated' and 'shadowed' from those introduced in § 2 (*a*).

The dashed lines in figure 3 represent curved rays in space on each of which the coordinates u_2 and u_3 have particular, constant values. On each ray the coordinate u_1 increases monotonically with distance from O. We partition S into a 'directly illuminated' part S_+ and a 'shadowed' part S_-. For a particular ray we denote the value(s) of u_1 at its intersection(s) with S by $u_{1(m)}$, where $m = 1, 2, \ldots, \hat{m}$. The $u_{1(m)}$ are ordered so that they increase monotonically with m. We consider the ray passing through a particular $P' \in S$, and we define $S_\pm$ by stating that when $P' \in S_+$ then $u_1' = u_{1(\hat{m})}$, whereas when $P' \in S_-$ then $u_1' = u_{1(\mu)}$ where $\hat{m}$ must be greater than μ. This is illustrated in figure 3.

Although details vary between the several separable coordinate systems (cf. Morse & Feshbach 1953, Chs 5, 6, 10, 11 [refer also to works by Flammer, by Meixner & Schäfke and by Watson quoted in (I)]; further useful details are given by Olver (1974) and Roseau (1976)), the dominant asymptotic behaviour of the radial eigenfunctions has the same general character for all systems. The asymptotic behaviour of $\hat{h}^{(2)}_{j,l}(\cdot)$ is described for small u_1 by

$$\hat{h}^{(2)}_{j,l}(u_1, k) \approx \gamma^{(1)}_{j,l}(l/\alpha u_1)^{l+1-\mu} \quad (k\alpha u_1 \ll l), \tag{2.9}$$

where $\mu = 0$ for rotational coordinate systems and $\mu = 1$ for cylindrical coordinate systems, and where α is the factor by which u_1 has to be multiplied to make αu_1 asymptotically equivalent to conventional metrical distance (refer to table 1). For large u_1 the asymptotic behaviour is characterized by

$$\hat{h}^{(2)}_{j,l}(u_1, k) = \gamma^{(2)}_{j,l}[1 + \beta_{j,l}(u_1, k)] \exp(-\mathrm{i}k\alpha u_1)/(k\alpha u_1)^{\nu} \quad (k\alpha u_1 > l), \tag{2.10}$$

where $\beta_{j,l}(\cdot)$ becomes increasingly negligible as $k\alpha u_1$ increases. Also, $\nu = 1$ for rotational coordinate systems and $\nu = \frac{1}{2}$ for cylindrical coordinate systems. The $\gamma_{j,l}$ are constants (refer to table 1). We denote by $\tilde{L}$ the maximum value of l for which the $\hat{h}^{(2)}_{j,l}(\cdot)$ can be approximated by (2.10), with $\beta_{j,l}(\cdot) = 0$, such that (2.6) is satisfied to within an error $\epsilon_{j,l}$, where each $|\epsilon_{j,l}|$ is less than a prescribed tolerance, ϵ say. The two types of asymptotic behaviour characterized by (2.9) and (2.10) lie on either side of $k\alpha u_1 = l$. It follows therefore that

$$\tilde{L} \leqslant k\alpha'_{1-} - \tilde{l}, \tag{2.11}$$

where the integer $\tilde{l}$ is a 'factor of safety'. Since, for a given ϵ, the value of $\tilde{l}$ depends upon the shape of S, there exists no general analytic means of estimating $\tilde{l}$. Computational experience must be relied on. Experience with spherical and cylindrical Bessel functions indicates that $\tilde{l} = 3$ is usually adequate, and that $\tilde{l} = 2$ often provides useful results.

TABLE 1. PARAMETERS IN ASYMPTOTIC EXPRESSIONS FOR $\hat{h}^{(2)}_{j,l}(u_1, k)$ IN SEVERAL SEPARABLE COORDINATE SYSTEMS

(Note that the $\gamma^{(1)}_{j,l}$ are valid when $l \gg kd$ for the elliptic cylinder coordinate system, and when $l \gg kd$ and $u_1 \gg 1$ for the prolate and oblate systems.)

coordinate system	$\gamma^{(1)}_{j,l}$	$\gamma^{(2)}_{j,l}$	α
circular cylinder	$-\mathrm{i}(2/\pi_l)^{\frac{1}{2}}(2/e)^l$	$(2\mathrm{i}/\pi)^{\frac{1}{2}}\mathrm{i}^l$	1
elliptic cylinder	$-\mathrm{i}l^{-\frac{1}{2}}(2/e)^l$	$(2\mathrm{i})^{\frac{1}{2}}\mathrm{i}^l$	d
spherical polars	$-\mathrm{i}l^{-1}(2/e)^{l+\frac{1}{2}}$	i^{l+1}	1
prolate spheroidal	$-\mathrm{i}l^{-1}(2/e)^{l+\frac{1}{2}}$	i^{l+1}	d
oblate spheroidal	$-\mathrm{i}l^{-1}(2/e)^{l+\frac{1}{2}}$	i^{l+1}	d

d = semifocal distance of the elliptic cylinder, prolate spheroidal, or oblate spheroidal coordinate systems.

It follows from (2.3), (2.4) and (2.6) that

$$\gamma^{(2)}_{j,l}\int_S\int f(\tau_1,\tau_2)\,\hat{Y}_{j,l}(u'_2,u'_3,k)\exp(-\mathrm{i}k\alpha u'_1)\,\mathrm{d}s/(k\alpha u'_1)^{\nu} \approx a_{j,l}+\epsilon_{j,l} \quad (l\in\{0\to\tilde{L}\},\, j\in\{-l\to l\}), \tag{2.12}$$

the form of which suggests that we make the substitution

$$\mathrm{d}s = \Delta(u'_2,u'_3)\,\mathrm{d}u'_2\,\mathrm{d}u'_3, \tag{2.13}$$

where $\Delta(\cdot)$ is found, in any particular case, by inspection of S. Note that it may not be possible to define $\Delta(\cdot)$ uniquely at points where S ceases to be analytic, but it is always possible to treat each analytic region of S piecewise and define $\Delta(\cdot)$ uniquely over each piece (the surface of bodies of physical interest cannot be so singular that they cannot be partitioned into denumerable analytic pieces). In general, $\Delta(\cdot)$ is not a single-valued function of u'_2 and u'_3 over all of S. But $\Delta(\cdot)$ is necessarily a single-valued function of u'_2 and u'_3 over S_+. We define our generalized physical optics surface source density $\tilde{f}$ to be zero over S_-:

$$\tilde{f} = \tilde{f}(u'_2,u'_3) = 0 \quad (P'\in S_-), \tag{2.14}$$

which means that, if we replace f in (2.12) by $\tilde{f}$, and if the particular application we are investigating allows us to treat an error of ϵ as negligible, we can immediately make use of (2.13) and arrive at

$$\gamma^{(2)}_{j,l}\int_{S_+}\int \tilde{f}(u'_2,u'_3)\,\hat{Y}_{j,l}(u'_2,u'_3,k)\exp(-\mathrm{i}k\alpha u'_1)\,\Delta(u'_2,u'_3)\,\mathrm{d}u'_2\,\mathrm{d}u'_3/(k\alpha u'_1) \approx a_{j,l} \quad (l\in\{0\to\tilde{L}\},\, j\in\{-l\to l\}). \tag{2.15}$$

The way in which S_+ is defined ensures that it spans continuously and single-valuedly the full ranges of u_2' and u_3', which means that the $\hat{Y}_{j,l}(u_2', u_3', k)$ are orthogonal over S_+, with a weight function, $w(u_2', u_3')$ say, that depends upon the particular coordinate system being used. It follows from (2.15) therefore that

$$(\Delta(u_2', u_3')/[w(u_2', u_3')\,(k\alpha u_1')^\nu])\exp(-\mathrm{i}k\alpha u_1')\,\tilde{f}(u_2', u_3') \approx \sum_{l=0}^{\tilde{L}}\sum_{j=-l}^{l}(a_{j,l}/\gamma_{j,l}^{(2)}\hat{I}_{j,l})\,\hat{Y}_{j,l}(u_2', u_3', k), \quad P' \in S_+, \tag{2.16}$$

where the $\hat{I}_{j,l}$ are the usual normalization constants. Both $\hat{I}_{j,l}$ and $w(\cdot)$ are given for the separable coordinate systems by Morse & Feshbach (1953, Chs 10 and 11).

Inspection of (2.10) indicates that, to within the tolerance to which (2.15) holds

$$((k\alpha u_1')^\nu/\gamma_{j,l}^{(2)})\exp(\mathrm{i}k\alpha u_1')$$

can be replaced in (2.16) by $1/\hat{h}_{j,l}^{(2)}(u_1', k)$. But reference to (2.9) indicates that $\hat{h}_{j,l}^{(2)}(u_1', k)$ becomes large everywhere on S_+ for all l somewhat greater than $\tilde{L}$. Recall that u_1' is defined to be single-valued in u_2' and u_3' on S_+. Consequently, the expression

$$\tilde{f}(u_2', u_3') = \frac{w(u_2', u_3')}{\Delta(u_2', u_3')}\sum_{l=0}^{\infty}\sum_{j=-l}\frac{a_{j,l}\hat{Y}_{j,l}(u_2', u_3', k)}{\hat{I}_{j,l}\hat{h}_{jl}^{(2)}(u_1', k)}, \quad P' \in S_+, \tag{2.17}$$

is often almost equivalent to (2.16). The terms for $l \leqslant \tilde{L}$ correspond closely to their equivalents in (2.16). The terms for $l \gg \tilde{L}$ are small, on account of (2.9). The terms for

$$l \in \{\tilde{L}+1 \to \tilde{L}+n\} \tag{2.18}$$

are appreciably in error. However, there seems to be no sure means of deciding *a priori* whether it is better to retain these terms or to discard them. We prefer to retain them because of the points raised in the following two paragraphs. The value of n depends in general upon the shape of S, but computational experience suggests that

$$\tilde{L}+n \geqslant k\alpha u_{1+}' + \tilde{l}. \tag{2.19}$$

When S itself coincides with a particular surface on which u_1 is constant then S_- is empty, S_+ is the whole of S and the $\hat{Y}_{j,l}(u_2', u_3', k)$ are orthogonal over S. If $\tilde{f}(\cdot)$, as given by (2.17), is substituted for $f(\cdot)$ in (2.3), we find on substituting (2.13) into (2.3) that (2.6) is satisfied identically for all $l \in \{0 \to \infty\}$, $j \in \{-l \to l\}$. Consequently, (2.17) is *exact* in such a case.

The formula on r.h.s. (2.17) is convenient because it can be computed straightforwardly without having to incorporate tests for the applicability of asymptotic expansions of the $\hat{h}_{j,l}^{(2)}(\cdot)$. Purely numerical considerations determine the formulae used for computing the $\hat{h}_{j,l}^{(2)}(\cdot)$ and the $\hat{Y}_{j,l}(\cdot)$, and the value of l at which the series is truncated.

(c) *Cylindrical physical optics*

When the scattering body is an infinite cylinder (of arbitrary cross-section) we use coordinates u_1, u_2 and z, where z is a Cartesian coordinate parallel to the cylinder axis. We denote the plane $z = 0$ by Ω, and the intersection of S with Ω by C. The subscripts appended to Ω and C correspond to those already appended to Υ and S.

Invoking the notation introduced in table 3 and § 2 (*a*) of (I), we write the incident field in the form

$$\psi_0 = \sum_{m=0}^{\infty}[c_m^{\mathrm{e}}a_m^{\mathrm{e}}\hat{J}_m^{\mathrm{e}}(u_1, k)\,\hat{Y}_m^{\mathrm{e}}(u_2, k) + c_m^{\mathrm{o}}a_m^{\mathrm{o}}\hat{J}_m^{\mathrm{o}}(u_1, k)\,\hat{Y}_m^{\mathrm{o}}(u_2, k)], \quad P \in \Omega, \tag{2.20}$$

where the superscripts e and o denote 'even' and 'odd' respectively. The generalized physical optics surface source density corresponding to (2.14) and (2.17) is

$$\begin{aligned}\tilde{F}(u_2') &= 0 \quad (P' \in C_-) \\ &= w(u_2')\frac{\mathrm{d}u_2'}{\mathrm{d}C}\sum_{m=0}^{\infty}\left[\frac{a_m^{\mathrm{e}}\hat{Y}_m^{\mathrm{e}}(u_2', k)}{\hat{I}_m^{\mathrm{e}}\hat{H}_m^{(2)\mathrm{e}}(u_1', k)} + \frac{a_m^{\mathrm{o}}\hat{Y}_m^{\mathrm{o}}(u_2', k)}{\hat{I}_m^{\mathrm{o}}\hat{H}_m^{(2)\mathrm{o}}(u_1', k)}\right], \quad P' \in C_+. \end{aligned} \tag{2.21}$$

The quantity $\mathrm{d}C/\mathrm{d}u_2'$ is equivalent to the quantity $\Delta(u_2', u_3')$ introduced in (2.13). The quantities u_1, u_2, $w(u_2)$ and $\hat{I}_m$ are listed in table 2 for circular and elliptic physical optics.

TABLE 2. QUANTITIES APPROPRIATE TO CYLINDRICAL PHYSICAL OPTICS

(The relevant wave functions are listed in table 3 of (I).)

	circular physical optics	elliptic physical optics
u_1, u_2	ρ, ϕ	ξ, η
$w(u_2)$	1	$(1-\eta^2)^{-\frac{1}{2}}$
$\hat{I}_m$	$2\pi,\ m = 0$ $\pi,\ m \neq 0$	$\int_{-1}^{1} S_{\times m}^2(kd, \eta)\, w(\eta)\, \mathrm{d}\eta$

$\times$ denotes either e or o.

3. IMPROVEMENT TO PHYSICAL OPTICS

Because physical optics surface source densities are calculated from only the incident field, they can be appreciably in error when S is concave. Multiple reflection is always significant within a concavity in the surface of a body. The more concave S is, the larger $(u_{1+}' - u_{1-}')$ tends to be, thereby increasing n, as follows from (2.11) and (2.19). But, an increase in n is equivalent to an increase in the number of terms in the summation on r.h.s. (2.17) that are significantly in error. So, both our physical intuition and our heuristic mathematical reasoning indicate that it is worth looking for an improvement to $\tilde{f}$ when the surface of the scattering body has indentations, especially if the associated computations turn out to be more economical than any known method of evaluating f by solving an integral equation. Any improvement that we find is likely to be useful for convex bodies as well.

When $\tilde{f}$, as given by (2.17), is substituted for f in (2.3), and (2.4) is used, it follows from (2.11), (2.19) and the definition of n that N of the $|b_{j,l} + a_{j,l}|$ will exceed ϵ, where

$$N = (2 + n + 2\tilde{L})\, n, \tag{3.1}$$

which is the number of expansion coefficients indexed by the integers j and l when

$$l \in \{\tilde{L} + 1 \to \tilde{L} + n\}.$$

We define an improved surface source density $\bar{f} = \bar{f}(\tau_1, \tau_2)$ over all of S by

$$\bar{f} = \tilde{f}_0 + h, \tag{3.2}$$

where $\tilde{f}_0 = \tilde{f}_0(u_2', u_3')$ is a physical optics source density incorporating those terms in the summation in (2.17) for which $l \in \{0 \to \tilde{L}\}$. The expansion coefficients differ from those in (2.17) for a reason made clear below. We define

$$\begin{aligned}\tilde{f}_0 &= 0 \quad (P' \in S_-) \\ &= \frac{w(u_2', u_3')}{\Delta(u_2', u_3')}\sum_{l=0}^{\tilde{L}}\sum_{j=-l}^{l}\frac{\tilde{a}_{j,l}\hat{Y}_{j,l}(u_2', u_3', k)}{\hat{I}_{j,l}\hat{h}_{j,l}^{(2)}(u_1', k)}, \quad P' \in S_+. \end{aligned} \tag{3.3}$$

The 'correction source density' $h = h(\tau_1, \tau_2)$ is defined by

$$h = \sum_{l=\tilde{L}+1}^{\tilde{L}+n} \sum_{j=-l}^{l} \alpha_{j,l} \Psi_{j,l}(\tau_1, \tau_2), \quad P' \in S, \tag{3.4}$$

where the $\alpha_{j,l}$ are expansion coefficients. The basis functions $\Psi_{j,l}$ are chosen for computational efficiency – refer to (6.3) of (I) *et seq.* Comparison of (3.1) and (3.4) shows that there are N of the $\alpha_{j,l}$.

The $\tilde{a}_{j,l}$ and the $\alpha_{j,l}$ are found, to the accuracy inherent in our definitions of $\tilde{L}$ and n, by substituting $\tilde{f}$ for f in (2.3) and invoking the null field equations (2.6). Use of (2.3), (2.4), (2.6), (2.10), (2.13), (2.14), (2.17) and (3.2) through (3.4) shows that

$$a_{j,l} = \sum_{l'=0}^{\tilde{L}} \sum_{j'=-l'}^{l'} \tilde{a}_{j',l'} \tilde{\Phi}_{j,j',l,l'} + \sum_{l'=\tilde{L}+1}^{\tilde{L}+n} \sum_{j'=-l'}^{l'} \alpha_{j',l'} \Phi_{j,j',l,l'} \quad (l \in \{0 \to \tilde{L}+n\}, j \in \{-l \to l\}), \tag{3.5}$$

where

$$\tilde{\Phi}_{j,j',l,l'} = \frac{\gamma^{(2)}_{j,l}}{\gamma^{(2)}_{j',l'} \hat{I}_{j',l'}} \int_{S_+} \int w(u'_2, u'_3)\, B_{j,j',l,l'}(u'_1, k)\, \hat{Y}_{j,l}(u'_2, u'_3, k)\, \hat{Y}_{j',l'}(u'_2, u'_3, k)\, \mathrm{d}u'_2\, \mathrm{d}u'_3 \tag{3.6}$$

and

$$B_{j,j',l,l'} = B_{j,j',l,l'}(u_1, k) = \frac{1 + \beta_{j,l}(u_1, k)}{1 + \beta_{j',l'}(u_1, k)} \tag{3.7}$$

and

$$\Phi_{j,j',l,l'} = \int_S \int \hat{h}^{(2)}_{j,l}(u'_1, k)\, \hat{Y}_{j,l}(u'_2, u'_3, k)\, \Psi_{j',l'}(\tau_1, \tau_2)\, \mathrm{d}s. \tag{3.8}$$

The reasoning presented between (2.10) and (2.11), together with (3.6), (3.7) and the orthogonality (with weight function w) over S_+ of the $\hat{Y}_{j,l}(\cdot)$, ensures that

$$\tilde{\Phi}_{j,j',l,l'} = \delta_{jj'} \delta_{ll'} + \epsilon_{j,j',l,l'} \quad (l, l' \in \{0 \to \tilde{L}\}), \tag{3.9}$$

where δ denotes the Kronecker delta and the $\epsilon_{j,j',l,l'}$ are of the order of ϵ. Note that $\epsilon_{j,j,l,l} = 0$. It follows from (3.5), therefore, to within the error (of order ϵ) implicitly allowed by the definition of $\tilde{L}$, that, for $l \leqslant \tilde{L}$,

$$a_{j',l'} = \tilde{a}_{j',l'} + \sum_{l''=\tilde{L}+1}^{\tilde{L}+n} \sum_{j''=-l''}^{l''} \alpha_{j'',l''} \Phi_{j',j'',l',l''} \quad (l' \in \{0 \to \tilde{L}\}, j' \in \{-l' \to l'\}), \tag{3.10}$$

which when substituted into (3.5), for $l > \tilde{L}$, gives

$$\hat{a}_{j,l} = \sum_{l'=\tilde{L}+1}^{\tilde{L}+n} \sum_{j'=-l'}^{l'} \alpha_{j',l'} \hat{\Phi}_{j,j',l,l'} \quad (l \in \{\tilde{L}+1 \to \tilde{L}+n\}, j \in \{-l \to l\}), \tag{3.11}$$

where

$$\hat{a}_{j,l} = a_{j,l} - \sum_{l'=0}^{\tilde{L}} \sum_{j'=-l'}^{l'} a_{j',l'} \tilde{\Phi}_{j,j',l,l'} \tag{3.12}$$

and

$$\hat{\Phi}_{j,j',l,l'} = \Phi_{j,j',l,l'} - \sum_{l''=\tilde{L}+1}^{\tilde{L}+n} \sum_{j''=-l''}^{l''} \Phi_{j'',j',l'',l'} \tilde{\Phi}_{j,j'',l,l''}. \tag{3.13}$$

We see from (3.12) and (3.6) that the $\hat{a}_{j,l}$ can be computed directly from the $a_{j,l}$ and the shape of the body. So, (3.11) is a system of N equations which can be solved for the N unknown $\alpha_{j,l}$ by elimination. Once the $\alpha_{j,l}$ are found, they are substituted into (3.10), immediately giving the $\tilde{a}_{j,l}$. Note that the latter would only equal the $a_{j,l}$ if the $\tilde{\Phi}_{j,j',l,l'}$ were all zero: this is why the expansion coefficients in (3.3) are different from those in (2.17). The improved surface source density $\tilde{f}$ is then obtained from (3.2) through (3.4).

The procedure which we have just described has considerable computational advantages. As we confirm in § 5, it can represent a significant improvement on physical optics, and it can

approach the accuracy obtainable with the full null field method. However, the unknown $\alpha_{j,l}$ are determined from a system of only N simultaneous, linear, algebraic equations; whereas $(\tilde{L}+1)^2+N$ equations are needed to evaluate the unknowns when the null field method is used in the form developed in (I).

The evaluation of $\bar{f}$ involves two main steps. First, there is the determination of the $\alpha_{j,l}$ from the inversion of a matrix of order N, requiring a number of operations proportional to N^3. Secondly, there is the determination of the $\tilde{a}_{j,l}$ by substituting the $\alpha_{j,l}$ into the $(\tilde{L}+1)^2$ equations (3.10), requiring a number of operations proportional to $(\tilde{L}+1)^2 N$. However, this can compare very favourably with the full null field method which requires a number of operations proportional to $\{(\tilde{L}+1)^2+N\}^3$.

In § 5 we present a computational example which illustrates this improved physical optics for a cylindrical body. We write the improved surface source density as

$$\bar{F}(C) = \tilde{F}_0(u_2') + H(C), \tag{3.14}$$

where $\tilde{F}_0$ is given by r.h.s. (2.21) truncated to $\tilde{M}+1$ even terms and $\tilde{M}$ odd terms, and with the a_m replaced by the $\tilde{a}_m$. The correction source density H is represented as

$$H(C) = \sum_{m=\tilde{M}+1}^{\tilde{M}+\tilde{N}} [\alpha_m^{\mathrm{e}} \Psi_m^{\mathrm{e}}(C) - \alpha_m^{\mathrm{o}} \Psi_m^{\mathrm{o}}(C)], \tag{3.15}$$

where the $\Psi_m(C)$ are chosen according to criteria discussed in § 6 (*b*) of (I). The evaluation of the $\tilde{a}_m$ and the α_m parallels that of the $\tilde{a}_{j,l}$ and the $\alpha_{j,l}$. The integers $2\tilde{M}+1$ and $2\tilde{N}$ respectively correspond, for cylindrical bodies, to the integers $\tilde{L}$ and n for arbitrarily shaped bodies.

4. Extinction deep inside body

It is shown in the references quoted in the paragraph containing (2.9) through (2.11) that, whatever separable coordinate system is employed, $|\hat{\jmath}_{j,l}(u_1, k)|$ decreases rapidly with increasing l, provided $k\alpha u_1 < L_1$, where $L_1 = L_1(u_1)$ is an integer which increases monotonically with ku_1. It is convenient to take L_1 as the largest value of l required for a multipole expansion to describe the total field to within a specified tolerance (e.g. of the order of ϵ). On replacing f in (2.3) by $\tilde{f}$ it follows from (2.1), and by analogy with (2.2), that

$$\psi_0 + \tilde{\psi} = \sum_{l=0}^{L_1} \sum_{j=-l}^{l} c_{j,l}[a_{j,l} + \tilde{b}_{j,l}^{-}] \hat{\jmath}_{j,l}(u_1, k)\, \hat{Y}_{j,l}(u_2, u_3, k). \quad P \in \Upsilon_{\mathrm{null}}, \tag{4.1}$$

where

$$\tilde{b}_{j,l}^{-} = -\int_{S_+}\int \tilde{f}(u_2', u_3')\, K_{j,l}^{-}\, \mathrm{d}u_2'\, \mathrm{d}u_3'. \tag{4.2}$$

We see that the value of L_1 depends upon the $a_{j,l}$ and the shape of S_+ as well as upon u_1 and k. But computational experience with fields expanded in eigenfunctions proper to spherical and cylindrical polar coordinates indicates that useful results are usually obtained if

$$L_1 \geqslant k\alpha u_1 + \tilde{l}, \tag{4.3}$$

where $\tilde{l}$ is introduced in (2.11). The point is that $|\hat{\jmath}_{j,l}(u_1, k)|$ decreases rapidly with increasing l when $k\alpha u_1 < (l - \tilde{l})$. Note that

$$L_1 < \tilde{L} \tag{4.4}$$

since $u_1 < u_{1-}'$ for $P \in \Upsilon_{\mathrm{null}}$.

Substituting (2.4) and (2.17) into (4.2), and using (2.10), (2.13), (3.6), (3.7) and (3.9), gives

$$\tilde{b}_{j,l}+a_{j,l}=-\sum_{l'=0}^{\tilde{L}}\sum_{j'=-l'}^{l'}a_{j',l'}\epsilon_{j,j',l,l'}-\sum_{l'=\tilde{L}+1}^{\infty}\sum_{j'=-l'}^{l'}a_{j',l'}Q_{j,j',l,l'}\quad(l\in\{0\to L_1\},\ j\in\{-l\to l\}),\tag{4.5}$$

where, for $l\leqslant L_1$ and $l'>\tilde{L}$,

$$Q_{j,j',l,l'}=\int_{S_+}\int\frac{w(u_2',u_3')\,\hat{h}^{(2)}_{j,l}(u_1',k)}{\hat{I}_{j',l'}\hat{h}^{(2)}_{j',l'}(u_1',k)}\,\hat{Y}_{j,l}(u_2',u_3',k)\,\hat{Y}_{j',l'}(u_2',u_3',k)\,\mathrm{d}u_2'\,\mathrm{d}u_3'.\tag{4.6}$$

On any S_+ whose behaviour is such that it can be a physically reasonable surface we can write

$$\hat{h}^{(2)}_{j,l}(u_1',k)/\hat{h}^{(2)}_{j',l'}(u_1',k)=\sum_{l''=0}^{\infty}\sum_{j''=-l''}^{l''}A_{j,j',j'',l,l'\,l''}\,\hat{Y}_{j'',l''}(u_2',u_3',k).\tag{4.7}$$

Since the $\hat{Y}_{j,l}(\cdot)$ are a complete set of functions orthogonal over S_+, with weight function $w(\cdot)$, we can also write

$$\hat{Y}_{j,l}(u_2',u_3',k)\,\hat{Y}_{j',l'}(u_2',u_3',k)=\hat{I}_{j',l'}\sum_{l''=0}^{\infty}\sum_{j''=-l''}^{l''}B_{j,j',j'',l,l',l''}\,\hat{Y}_{j'',l''}(u_2',u_3',k)/\hat{I}_{j'',l''}.\tag{4.8}$$

Substitution of (4.7) and (4.8) into (4.6) gives

$$Q_{j,j',l,l'}=\sum_{l''=0}^{\infty}\sum_{j''=-l''}^{l''}A_{j,j',j'',l,l',l''}\,B_{j,j',j'',l,l',l''}.\tag{4.9}$$

In general we can expect the $|A_{j,j',j'',l,l',l''}|$ to decrease rapidly with increasing l'', for l'' greater than some particular integer $\hat{l}$. The smoother S_+ is, the smaller $\hat{l}$ will be.

Whatever coordinate system is being used, the $|B_{j,j',j'',l,l',l''}|$ are largest for values of l'' close to $|l'\pm l|$. If $|l'-l|<\hat{l}$, all terms in the summation on r.h.s. (4.9) are small, so that $Q_{j,j',l,l'}$ is small. Inspection of (3.7) and the references quoted for (2.10) shows that $|\epsilon_{j,j',l,l'}|$ decreases as $l'-l$ increases. Consequently, both double summations in (4.5) are small when L_1 is small enough, which is the same as u_1 being small enough. This demonstrates that

$$\tilde{b}^{-}_{j,l}+a_{j,l}\approx 0\tag{4.10}$$

for all significant values of j and l for points P far enough inside $\mathcal{V}_{\mathrm{null}}$. But the condition laid on $\tilde{b}^{-}_{j,l}$ by (4.10) is the same as that laid on the $b^{-}_{j,l}$ by the exact null field equations (2.6).

We see then that the deeper we penetrate inside the body, the more nearly does the generalized physical optics satisfy the extinction theorem. This is an extension of our previous finding that the differences between the true and the planar physical optics far fields scattered from a roughened flat surface are likely to be less than the differences between the corresponding near fields (Bates 1975*a*).

5. Applications

We present surface source densities on, and far fields scattered from, cylindrical bodies having the cross sections shown in figure 4. We compare results computed by both the general null field method developed in (I) and the physical optics approximations introduced here. We examine planar physical optics, circular physical optics and elliptic physical optics (refer to table 2). All computational details accord with what is described in § 6 (*c*) of (I).

We compute scattered far fields either by substituting (2.10) into (2.2), or by evaluating the integral in (2.7); remembering that, for cylindrical coordinate systems, $b^{+}_{j,l}$ and $f(\tau_1,\tau_2)$ become

b_m^+ and $F(C)$, respectively, and the double integral in (2.7) reduces to a single integral. When computing physical optics fields we replace b_m and F by $\tilde{b}_m$ and $\tilde{F}$ respectively.

We take ψ_0 to be a plane wave incident at an angle φ. Recall from (I) that we use the symbol C to denote both the curve and the distance along it. We denote by $\bar{C}$ the value of C at the point on C where $\phi' = \varphi$. Inspection of figure 4 shows that there is only one such point for any of the scattering bodies which we investigate.

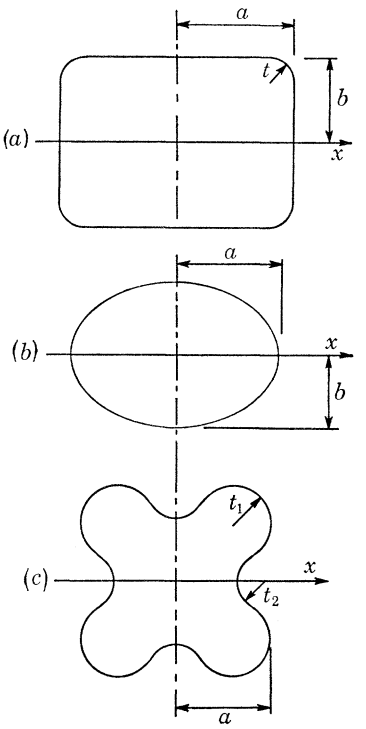

FIGURE 4. Cylindrical scattering bodies: (*a*) rectangular cylinder with rounded corners; (*b*) elliptical cylinder; (*c*) cylinder with concavities.

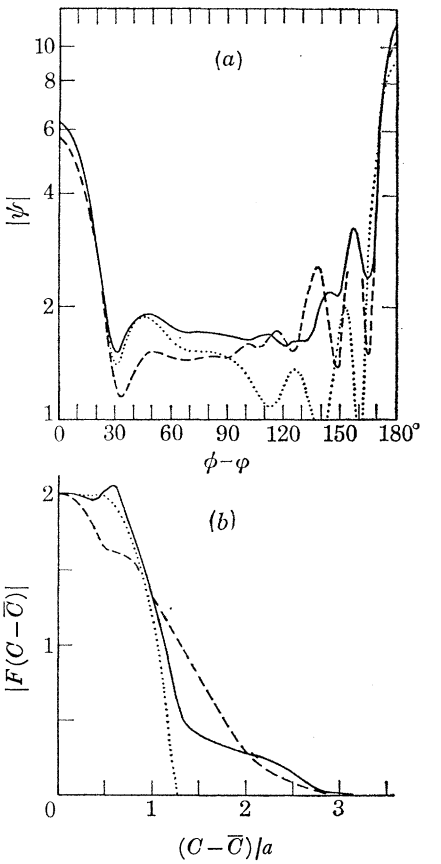

FIGURE 5. Scattered far fields (*a*) and surface source densities (*b*) for a square cylinder with rounded corners (refer to figure 4 (*a*)). $\varphi = 0$, $a = 1.5\lambda$, $b = a$, $t = 0.5a$; ——, circular null field method; – – –, circular physical optics; ....., planar physical optics.

Because of the symmetries possessed by the cylinders shown in figure 4, the scattered fields are symmetrical about $\phi = \varphi$ and the surface source densities are symmetrical about $C = \bar{C}$, provided that φ is chosen to be an integral multiple of $\frac{1}{2}\pi$. We take advantage of this and, consequently, only compute fields and surface sources over half their full ranges. In our graphs we only show the magnitudes of fields and surface source densities. But remember that the phase as well as the magnitude of a surface source density affects the corresponding scattered field. So, when the magnitude of the latter is accurate, to within some useful tolerance, then the phase of the former must be similarly accurate.

In figures 5 through 13 we present typical results for bodies having the cross sections shown in figure 4. When computing the solid curves in figures 8 and 9, we chose the semi-focal distances

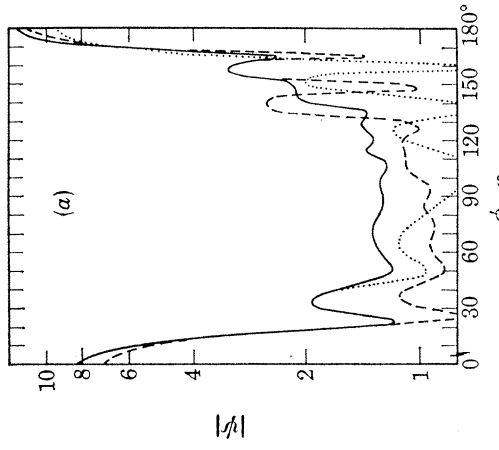

FIGURE 6. Scattered far fields (*a*) and surface source densities (*b*) for a square cylinder with rounded corners (refer to figure 4 (*a*)). $\varphi = 0$, $a = 1.5\lambda$, $b = a$, $t = 0.25a$; ——, circular null field method; – – –, circular physical optics; ……, planar physical optics.

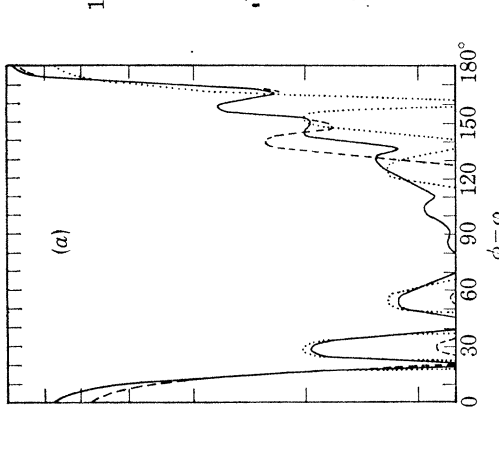

FIGURE 7. Scattered far fields (*a*) and surface source densities (*b*) for a square cylinder (refer to figure 4 (*a*)). $\varphi = 0$, $a = 1.5\lambda$, $b = a$, $t = 0$; ——, circular null field method; – – –, circular physical optics; ……, planar physical optics.

FIGURE 8. Scattered far fields (*a*) and surface source densities (*b*) for an elliptical cylinder (refer to figure 4 (*b*)). $\varphi = \frac{1}{2}\pi$, $a = 1.5\lambda$, $b = 0.8a$; ——, elliptic physical optics; – – –, circular physical optics; ……, planar physical optics.

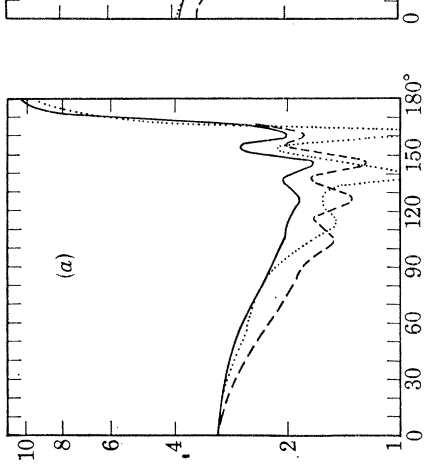

FIGURE 9. Scattered far fields (*a*) and surface source densities (*b*) for an elliptical cylinder (refer to figure 4 (*b*)). $\varphi = \frac{1}{2}\pi$, $a = 1.5\lambda$, $b = 0.5a$; ——, elliptic physical optics; – – –, circular physical optics; ……, planar physical optics.

PHILOSOPHICAL TRANSACTIONS OF THE ROYAL SOCIETY A MATHEMATICAL, PHYSICAL & ENGINEERING SCIENCES

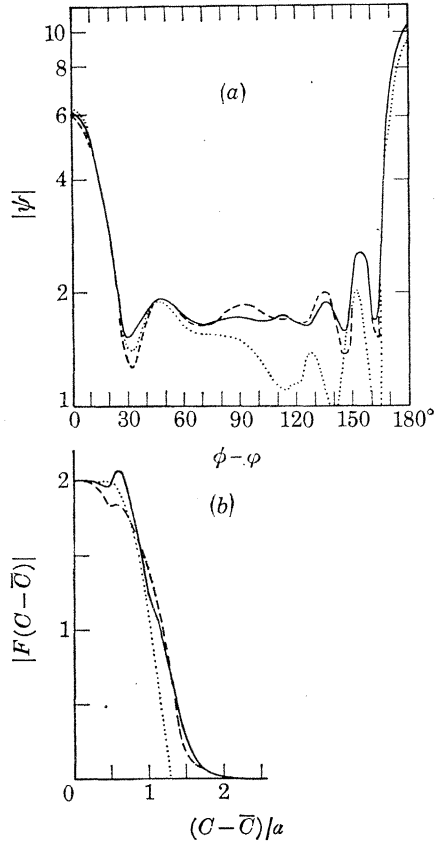

FIGURE 10. Scattered far fields (*a*) and surface source densities (*b*) for a rectangular cylinder with rounded corners (refer to figure 4 (*a*)). $\varphi = \frac{1}{2}\pi$, $a = 1.5\lambda$, $b = 0.5a$, $t = 0.5a$; ——, elliptic null field method; – – – elliptic physical optics; ……, planar physical optics.

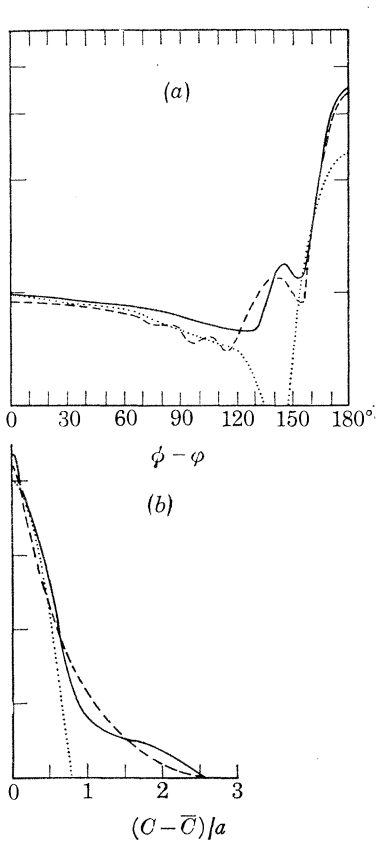

FIGURE 11. Scattered far fields (*a*) and surface source densities (*b*) for a rectangular cylinder with rounded corners (refer to figure 4 (*a*)). $\varphi = 0$, $a = 1.5\lambda$, $b = 0.5a$, $t = 0.5a$; ——, elliptic null field method; – – –, elliptic physical optics; ……, planar physical optics.

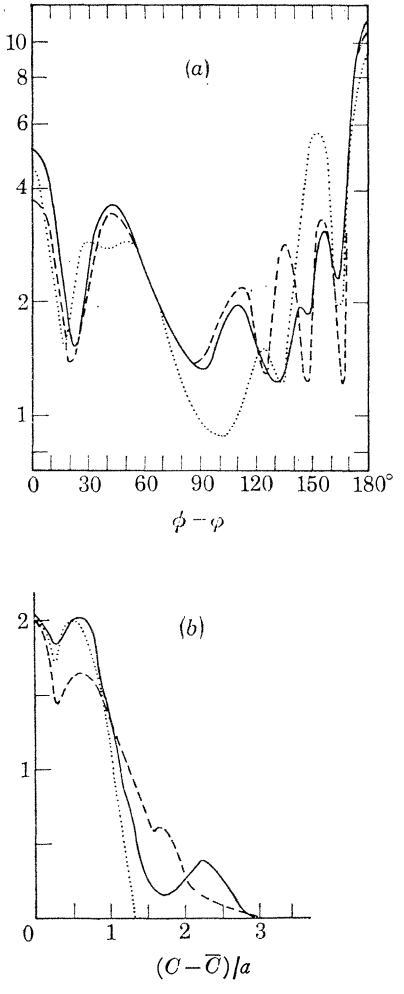

FIGURE 12. Scattered far fields (*a*) and surface source densities (*b*) for a cylinder with concavities (refer to figure 4 (*c*)). $\varphi = 0$, $a = 1.5\lambda$, $t_1 = 0.5a$, $t_2 = 0.5a$; ——, circular null field method; – – –, circular physical optics; ……, planar physical optics.

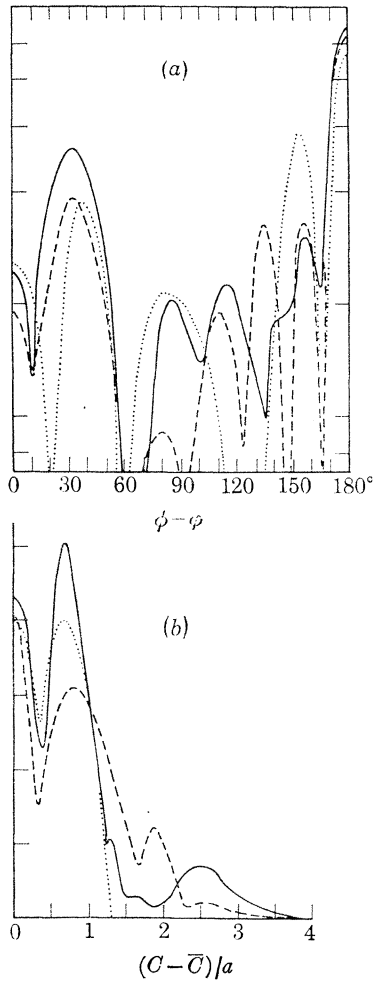

FIGURE 13. Scattered far fields (*a*) and surface source densities (*b*) for a cylinder with concavities (refer to figure 4 (*c*)). $\varphi = 0$, $a = 1.5\lambda$, $t_1 = 0.4a$, $t_2 = 0.3a$; ——, circular null field method; – – –, circular physical optics; ……, planar physical optics.

of our elliptic cylinder coordinates to be the same as the semi-focal distances of the scattering bodies. Consequently, elliptic physical optics is exact for figures 8 and 9, so that the solid curves can be assumed accurate, to within the tolerance set by our draughtsmanship. When computing the solid curves in figures 10 and 11, we chose the semi-focal distances of our elliptic cylinder coordinates such that Υ_{null} occupied as much of Υ_{-} as possible: refer to § 8 (*b*) of (I). Consequently, we are confident on account of the results we have already reported in (I) that the solid curves in figures 10 and 11 are accurate, to within the tolerance set by our draughtmanship.

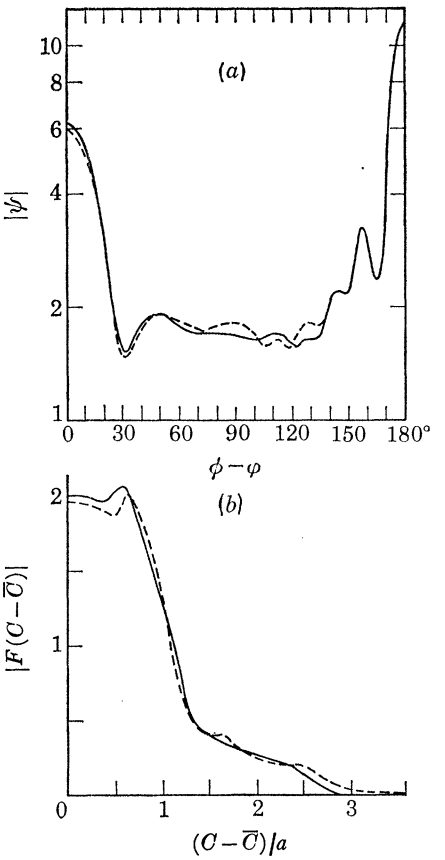

FIGURE 14. Scattered far fields (*a*) and surface source densities (*b*) for a square cylinder with rounded corners (refer to figure 4 (*a*)). $\varphi = 0$, $a = 1.5\lambda$, $b = a$, $t = 0.5a$; ——, circular null field method; – – –, improved circular physical optics $\tilde{N} = 11$, $\tilde{M} = 7$.

Figure 14 shows the result of applying our improvement to physical optics (see § 3) to a rectangular cylinder with rounded corners. The differences between the accurate and approximate computations are almost negligible for most practical applications, and yet $\tilde{N}$ was 11 while $\tilde{N}+\tilde{M}$ was 18. We did not need to compute any odd wave functions because of the symmetry of the scattering body. We point out that the computational economy of the approximate over the exact method would be more marked for an asymmetrical body.

6. Conclusions

A striking aspect of the computed results we present in § 5 is that our new physical optics can make recognizable, and sometimes accurate, predictions of the surface source densities in the umbra and penumbra of scattering bodies. Our formulae (2.14) and (2.16) can always be applied straightforwardly, without the tedious precautions which seem to be unavoidable in general with either Fock theory (cf. Goodrich 1959) or the geometrical theory of diffraction – for bodies of complicated shape the latter can, of course, provide more accurate results.

When comparing our new physical optics methods with planar physical optics we see that they always predict forward scattered fields more accurately. They tend to be superior for all scattering directions except close to the actual back scattering direction. Even for specular scattering from a body with a flat surface, for which planar physical optics is ideal, our new physical optics is not much inferior (refer to figure 7).

Our results suggest that it is important to use the type of physical optics most appropriate for the body in question. As we have reported in (I), the efficiency of the null field method improves as Υ_{null} spans more of Υ_{-}, or Ω_{null} spans more of Ω_{-}. We conjecture that the same criterion should be applied to the choice of the physical optics method.

In geometrical optics, and in Kirchhoff's approach to diffraction theory, the directly illuminated and shadowed parts of a body are found by examining both the incident field and the body. In § 2 (*b*) we introduce a definition which depends only upon the shape of the surface of the body. It is this which allows us to predict the surface source density in the umbra and penumbra. We suggest that our new definition of 'illuminated' and 'shadowed' might be more useful in general. For instance, it may prove possible to replace planar physical optics with an asymptotic form of spheroidal physical optics, obtained by taking the semi-focal distance of the spheroidal coordinates to be arbitrarily large compared with the wavelength. This would have the advantage that the asymptotic property established in § 4 would then apply to a Kirchhoff-type theory appropriate for extended rough surfaces.

The improvement introduced in § 3 may be very significant computationally, on two counts. First, it is a step towards developing accurate methods which are much more efficient than the rigorously based methods, and yet are straightforwardly related to them theoretically (the geometrical theory of diffraction is very powerful but it is usually extremely difficult, in specific cases, to determine the order of the differences between it and exact theory). Secondly, it is the kind of approach from which may come useful *a priori* assessments of the orders of the matrices which must be inverted to solve particular direct scattering problems to required accuracies – as Jones (1974) and Bates (1975 *b*) point out, this is probably the outstanding computational problem area for diffraction theorists.

One of us, D. J. N. Wall, acknowledges the support of a New Zealand University Grants Committee Postgraduate Scholarship.

References

Bates, R. H. T. 1968 Modal expansions for electromagnetic scattering from perfectly conducting cylinders of arbitrary cross section. *Proc. IEE* **115**, 1443–1445.

Bates, R. H. T. 1975*a* New justification for physical optics and the aperture-field method. *Proc. XXth AGARD Meeting on Electromagnetic Wave Propagation Involving Irregular Surfaces and Inhomogeneous Media*. The Hague, Netherlands; AGARD Conf. Publication no. CPP-144, pp. 36-1 to 36-7.

PHILOSOPHICAL TRANSACTIONS OF THE ROYAL SOCIETY A MATHEMATICAL, PHYSICAL & ENGINEERING SCIENCES

Bates, R. H. T. 1975*b* Analytic constraints on electromagnetic field computations. *IEEE Trans. Microwave Theory Tech.* MTT-**23**, 605–623.
Bates, R. H. T. & Wall, D. J. N. 1977 Null field approach to scalar diffraction: I. General method. *Phil. Trans. R. Soc. Lond.* A **287**, 45–78. (Preceding paper).
Beckmann, P. & Spizzichino, A. 1963 *The scattering of electromagnetic waves from rough surfaces*. New York: Macmillan (Pergamon).
Bouwkamp, D. J. 1954 Diffraction theory. *Rep. Prog. Phys.* **17**, 35–100.
Crispin, J. W. & Maffett, A. L. 1965 Radar cross-section estimation for simple shapes. *Proc. IEEE* **53**, 833–848.
Goodrick, R. F. 1959 Fock theory – an appraisal and exposition. *Trans. IRE* AP-7, Special issue, S28–S36.
Jones, D. S. 1974 Numerical methods for antenna problems. *Proc. IEE* **121**, 573–582.
Kouyoumjian, R. G. 1965 Asymptotic high-frequency methods. *Proc. IEEE* **53**, 864–876.
Morse, P. M. & Feshbach, H. 1953 *Methods of theoretical physics*. New York: McGraw-Hill.
Olver, F. W. J. 1974 *Asymptotics and special functions*. New York and London: Academic Press.
Roseau, M. 1976 *Asymptotic wave theory*. Amsterdam and Oxford: North-Holland.
Senior, T. B. A. 1965 A survey of analytical techniques for cross-section estimation. *Proc. IEEE* **53**, 822–833.
Ursell, F. 1966 On the rigorous foundation of short-wave asymptotics. *Proc. Camb. Phil. Soc.* **62**, 227–244.

PHILOSOPHICAL TRANSACTIONS OF THE ROYAL SOCIETY A MATHEMATICAL, PHYSICAL & ENGINEERING SCIENCES